Electronic Supplementary Information

Illuminating the nature and behavior of the active center: the key for photocatalytic H_2 production in Co@NH_2-MIL-125(Ti)

Ana Iglesias-Juez[a]*, Sonia Castellanos[b]*, Manuel Monte[c], Giovanni Agostini[c†], Dmitrii Osadchii[d], Maxim A. Nasalevich[d], Alma I. Olivos Suarez[d], Sergey L. Veber[e], Matvey V. Fedin[e], Jorge Gascón[d,f]

[a] Instituto de Catálisis y Petroleoquímica, CSIC, 28049 Madrid, Spain.

[b] Advanced Research Center for Nanolithography,1090 BA Amsterdam, The Netherlands.

[c] European Synchrotron Radiation Facility, 38043 Grenoble Cedex 9 France.

[d] Catalysis Engineering, Applied Sciences, Delft University of Technology, Julianalaan 136, 2628 BL, Delft, The Netherlands.

[e] International Tomography Center SB RAS, and Novosibirsk State University, Novosibirsk 630090, Russia.

[f] King Abdullah University of Science and Technology, KAUST Catalysis Center, Advanced Catalytic Materials, Thuwal 23955, Saudi Arabia.

Present Addresses:

† Leibniz-Institut für Katalyse e. V. an der UniVersität Rostock, Albert-Einstein-Strasse 29a, D-18059 Rostock.

In situ and *operando* X-ray absorption spectroscopy experiments

Photo-cell

This type of experiment required a well-designed setup where the intrinsic noise of a suspended sample in a liquid could be minimized and a homogeneous and sufficient illumination with external visible light source could be applied on the sample in order to induce photocatalytic reactions.

Some cells for kind of *in-situ* studies of photoheterogeneous catalysts have been previously reported. In those cases, the reaction took place in a photoreactor from which samples were extracted and analyzed in a semi-dynamic fashion.[1,2] Similarly, in transient XAS, excitation of the system is performed in a different cell compartment that the XAS measurement.[3]

To perform the measurements under *in situ* realistic conditions, avoid sample loss during circulation and record also XAS of the photo stationary state, we designed a cell where visible light was shone through a back quartz window while X-ray fluorescence spectroscopy was recorded simultaneously through a front kapton window. The volume of the cell was optimized to accommodate a thin layer of stirred colloidal suspension that could be homogeneously illuminated with divergent visible light emitted from an optical fiber. A similar cell was used to investigate thin films of CuO/TiO_2.[4] However, in that case the TiO_2 was deposited on an ITO electrode that acted as a window for visible

light illumination. To the best of our knowledge this is the first time that the active site of a photocatalytic MOF is studied by in-situ XAS.

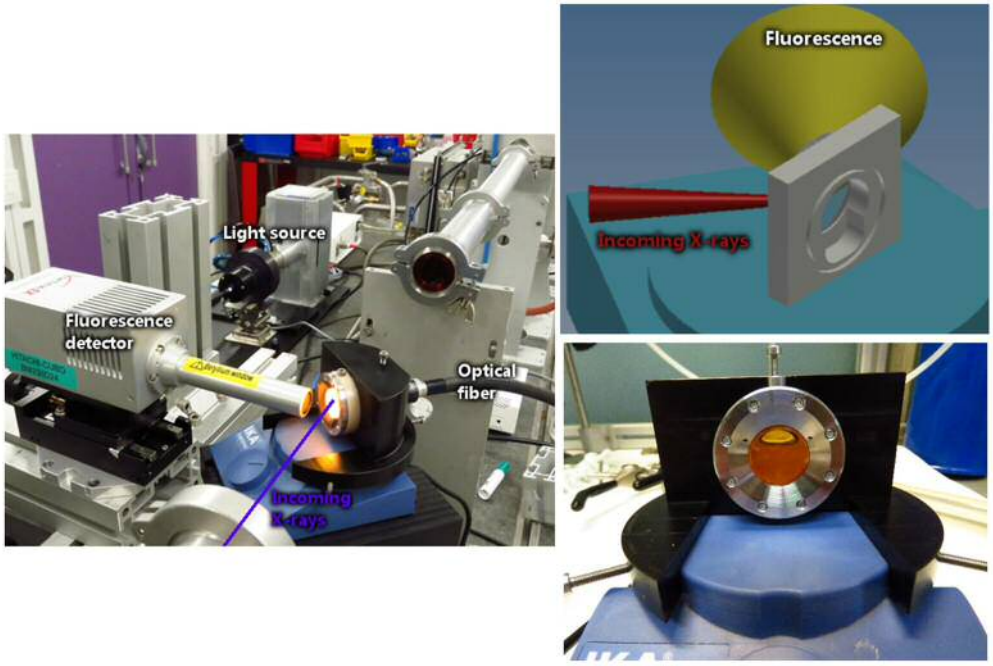

Fig. S1. Experimental set up. Details of the design cell for *in situ* measurement under external illumination.

Reaction conditions

For the photocatalytic synchrotron experiments, Co@MOF (5.0 mg) was suspended in a mixture of acetonitrile (5 mL), triethylamine (1 mL) and deionized water (0.1 mL) and the suspension degassed by bubbling nitrogen for 10 min while stirring. The resulting suspension was transferred (under nitrogen atmosphere) to the above described *in situ* photocell (head space approximately 1 mL), continuing under stirring and was purged with nitrogen beforehand. For the irradiation, a 300 W Hg/Xe lamp coupled with an IR filter (circulating water; ca. 10 cm path length) and a 408 nm UV cut-off filter was used. After, an electronic shutter provides a TTL input (via BNC) allowing to drive the shutter from another source. Thus, the open/close switch was synchronized and triggered with XANES acquisition. Then, there was an optic focusing assemblies that focus the collimated light into a 2 m fiber since the light source setup was far from the cell and the fiber allowed a direct focus of the visible light into the quartz window of the photocell. The fiber probe used here is a Liquid Light Guide with high transmittance (around 80%). At the end, a focusing lens, which has a working distance of 1 cm, illuminated the suspension through the quartz window.

Instrumentation

XAS data was collected at BM23 beamline[5] of the European Synchrotron Radiation Facility, ESRF, Grenoble (the ring energy was 6.0 GeV and the current 150–200 mA). Two crystals of Si(111) were used as a monochromator and a pair of Si-coated mirrors with a glancing angle of 3 mrad were employed to reject high-energy harmonics. Spectra in transmission were recorded with ionization chambers filled at 2 bar with a N_2/He mixture with appropriate ratio to obtain an absorption of 0.3 in the I0 and 0.7 in both I1 and I2 (this last is used for a simultaneously reference record). Spectra in fluorescence were recorded with a silicon Vortex detector placed at 90º with respect to the incident X-ray beam. Beam size at sample was 5 mm in horizontal and 0.2 mm in vertical.

XANES and EXAFS spectra were taken integrating 2 s per point of a mesh divided in three regions: steps of 5 eV were applied in the pre-edge, 0.3 eV steps around the energy of the edge and longer steps above the edge to obtain a

constant space between points in k-space (0.03 $Å^{-1}$). Each EXAFS spectrum was repeated three times and data averaged to obtain a better signal-to-noise ratio.

Data analysis

XANES: spectra normalization

Spectra normalization was performed with Athena program, part of Demeter package 0.9.21.[6] The spectra of all samples and references (CoO, $CoBr_2$, etc.) were shift-corrected using an external Co foil reference which was measured between samples.

The assignation of the oxidation state was performed evaluating the first derivative of normalized XANES spectra for Co@MOF and references of the oxidation states: Co(0), Co(II) and Co(III) (See Fig. S2).

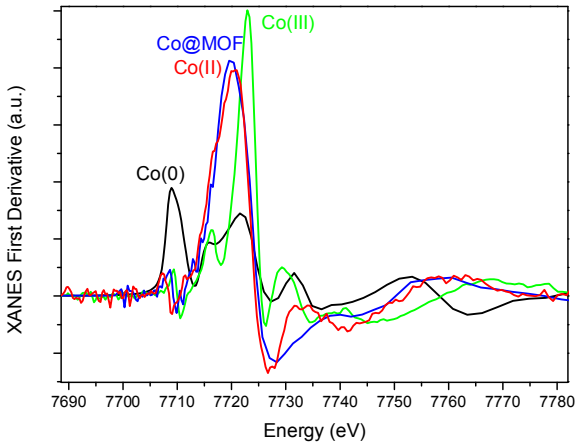

Fig. S2. First derivative of normalized XANES spectra for Co@MOF and references of the oxidation states: Co(0), Co(II) and Co(III).

The XANES spectra obtained for the different references are presented in Fig. S3.

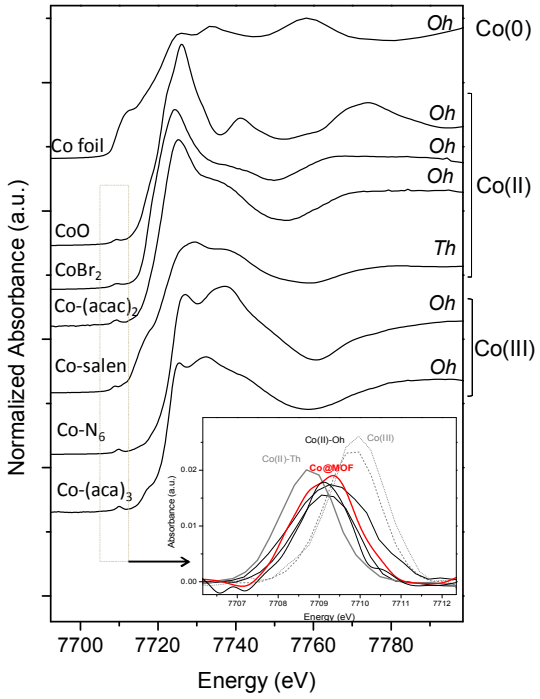

Fig. S3. XANES spectra for standard references of (0), (II) and (III) oxidation state. The labels *Oh* and *Th* refer to octahedral and tetrahedral environments respectively.

In order to evaluate the possible formation of a cobaloxime complex within the structure of the MOF, this reference was also measured in different suspensions (Fig. S4).

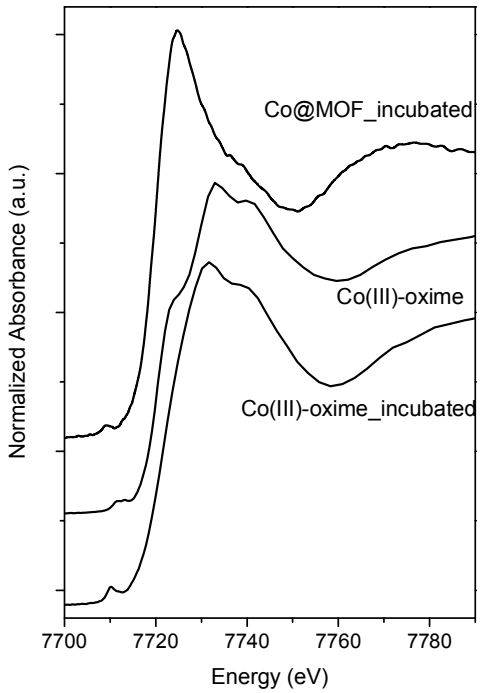

Fig. S4. XANES spectra of the Co(III)-cobaloxime complex in AN and AN-TEA-H_2O suspensions. XANES spectrum of Co@MOF in AN-TEA-H_2O suspension is also included.

EXAFS fitting

Artemis program, also part of Demeter package 0.9.2166, was used for EXAFS deconvolution. The fitting of χ(k) were performed for all samples and references in three k-weights (χ(k)·k, χ(k)·k^2 and χ(k)·k^3, simultaneously, in order to correctly represent both the light and the heavy atoms. Paths phases and amplitudes were calculated, for all models, with the Feff6 program contained in Artemis. Appropriate limits for the Hanning windows in k and R spaces were chosen for each spectrum. For the k-space one, the result of the Fourier Transform (to R-space) was compared increasing the range of the k-space window from the lower acceptable value (7 A^{-1}) to the highest possibility (13 A^{-1} in the case of CoO); the wider window which not include obviously non-real features was selected. For the R-space, a minimum (close to zero) of the magnitude at a distance which includes all fitting shells was selected. Amplitude reduction factor (S_0^2=0.88±0.04) was calculated over reference CoO and applied to all other spectra. Only for this spectrum two-, three and four-legs paths were taken into account as an effort to obtain the better value of S_0^2; all other spectra were fit with only single-scatter paths. Same energy shift (ΔE_0) was chosen for all paths of the same spectra.

Fig. S5 displays the fitted Fourier transforms of the Co k^2-weighted spectra for Co@MOF before and after incubation periods.

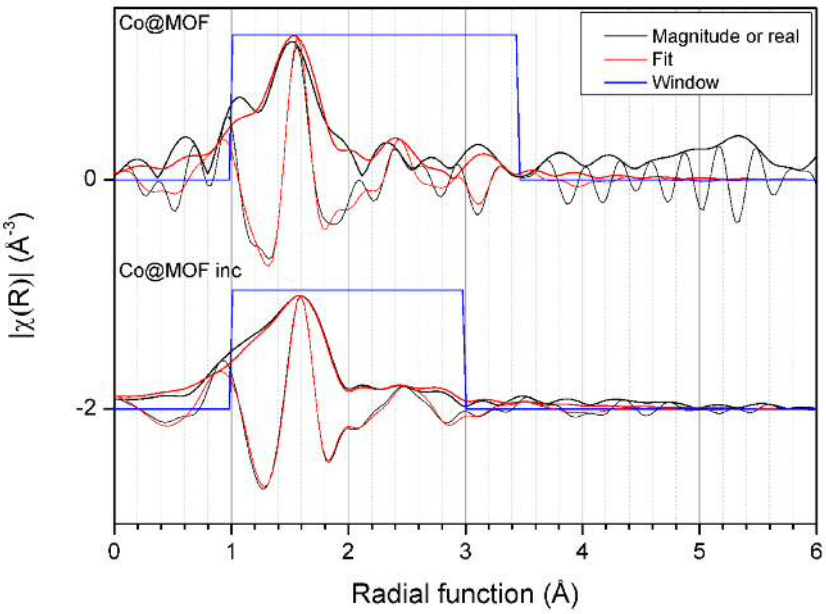

Fig. S5. Experimental and fitted k^2-weighted modulus and real part of the Fourier transform of Co K-edge EXAFS spectra corresponding to Co@MOF before and after incubation period. Structural parameters derived from EXAFS analysis in table S.1.

Table S1. Complementary structural parameters, mean-square disorder in the distribution of interatomic distances (σ^2) and energy shift (E_0) derived from analysis of the EXAFS data in Fig. 2. K_{region} [3-12].

Co@MOF-fresh				
Path	*N*	*R*	σ^2	E_0
Co-O	5.9±0.9	2.14±0.04	0.0042±0.0008	1±0.3
Co-N	-	-	-	-
Co-Br	0.5±0.3	2.45±0.03	0.0040±0.002	1±0.3
Co-Co	0.8±0.4	3.39±0.05	0.006±0.003	1±0.3
Co-Ti	-	-	-	-
Co@MOF-12 h incubation				
Co-O	3.9±0.2	2.05±0.07	0.005±0.001	0.5±0.7
Co-N	2.0±0.3	1.98±0.05	0.005±0.002	0.5±0.7
Co-Br	0.3±0.2	2.68±0.06	0.004±0.002	0.5±0.7
Co-Co	0.6±0.5	2.93±0.07	0.005±0.003	0.5±0.7
Co-Ti	0.3±0.2	3.20±0.10	0.007±0.002	0.5±0.7
Co@MOF-24 h incubation				
Co-O	3.8±0.2	2.052±0.002	0.005±0.002	-4.1±0.2
Co-N	1.5±0.3	1.934±0.006	0.005±0.002	-4.1±0.2
Co-Br	-	-	-	-
Co-Co	0.3±0.2	2.84±0.03	0.003±0.002	-4.1±0.2
Co-Ti	0.8±0.2	3.08±0.02	0.007±0.002	-4.1±0.2

Fig. S6 displays the Fourier transforms of the Co k^2-weighted spectra for $CoBr_2$ and Co-oxime references.

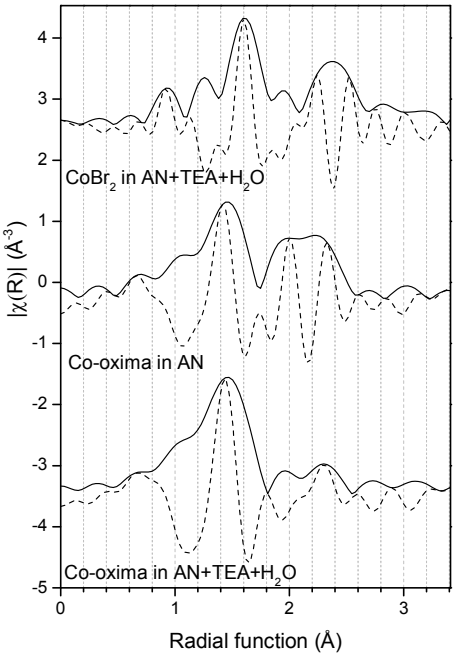

Fig. S6. Fourier transforms of the Co k^2-weighted spectra of $CoBr_2$ and the Co(III)-cobaloxime complex in AN and AN-TEA-H_2O suspensions.

***Operando* experiments during light ON-OFF switchings**

After the incubation period, the suspension of Co@MOF in the reaction media (acetonitrile/trietilamine/H_2O, N_2 purged) was illuminated with external visible light (>400 nm) during 6 h (reaction conditions). Next, the light was switched off for another equal period. This cycle was repeated to check reproducibility. XANES spectra were continuously acquired to follow the process. Fig. S7 displays a schematic representation of the experiment.

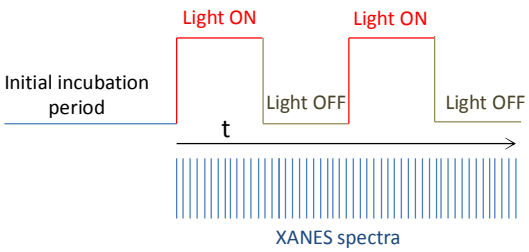

Fig. S7. A schematic representation of the *operando* experiments during light ON-OFF switchings.

Fig. S8 presents the normalized spectra during the first step with the light ON. The illumination induced a shift of the XANES edge toward lower energies and a decrease of the white line intensity (at 7725 eV) and the shoulder around 7737 eV. Differential mode analysis allows a more detailed exam. Thus the initial spectrum under dark conditions was subtracted from each of the following spectrum.

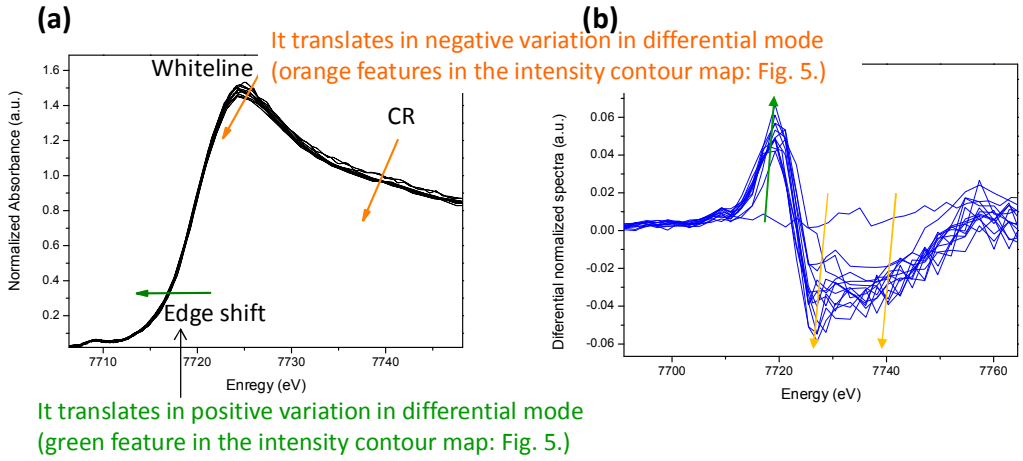

Fig. S8. (a) Normalized XANES spectra during the first step with the light on. (b) Differential spectra.

The shape of the pre-edge features does not change which would indicate that there are no modifications of the local Co environment, nor changes by re-hybridization. The shift of the absorption edge towards lower energies is an indication of partial reduction of the Co centers. In addition, this is support by the concomitant decrease in the white line intensity and the shoulder around 7737 eV, attributed to an electron density increase of the p and d states, respectively, involved in the 1s–4sp and 1s-3d resonance transitions. Therefore, the results point to a charge transfer directly into p and d(eg) states.

EPR measurements

EPR measurements were carried out in continuous wave mode at X-band (9 GHz) and Q-band (34 GHz) using a commercial EPR spectrometer Bruker Elexsys E580 equipped with an Oxford Instruments temperature control system (T = 4–300 K). Samples were prepared by suspending Co@MOF in a solution of electron donor TEA/CH_3CN/H_2O. The volume of suspension placed into the EPR resonator was 50–60 mL. Each sample was degassed by several freeze–pump–thaw procedures and then sealed. The illumination was accomplished using LED with 380 nm light.

Fig. S9a and S9b show the Gaussian fitting of the X- and Q-band EPR spectra of photoinduced signal in Co@MOF. One observes that EPR line shape is closely Gaussian with only minor deviations.

Fig. S9c shows the normalized Q-band EPR spectra at T=40-190 K. The line shapes weakly depend on temperature; only slight narrowing at high temperatures is observed due to the more efficient exchange narrowing.

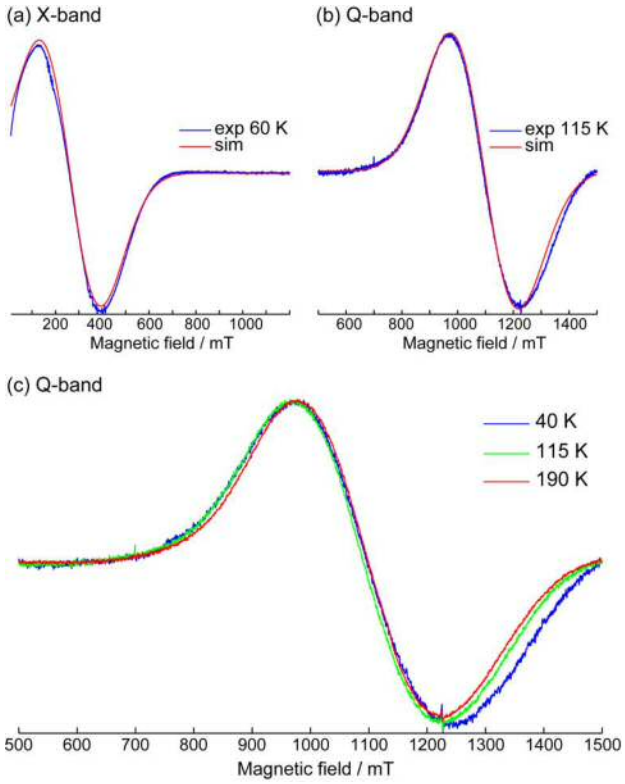

Fig. S9. EPR spectra of Co@MOF in reaction mixture $CH_3CN/TEA/H_2O$ upon irradiation at 380 nm for 19 h. (a) X-band EPR spectrum at 60 K and Gaussian fitting (g~2.65, Γ_{pp}~300 mT); (b) Q-band EPR spectrum at 115 K and Gaussian fitting (g~2.23, Γ_{pp}~300 mT); (c) normalized Q-band EPR spectra at several temperatures (as indicated).

Photocatalytic tests on Co@MOF systems with other metallic nodes in the framework

The participation of Ti in the active site formation was proved when photocatalyitc tests on other MOFs based on the same amino functionalised linker was loaded with Co using the same protocol as reported in ref. [7]. Experimental setup consisted of a 500 W Xe/Hg lamp (66983, Newport), a custom-made Pyrex-glass reactor, a CP 9001 gas chromatograph (Chrompack) for analysis of the headspace, and a KSLA gas pump and the light source. The reactor has a volume of 42.1 mL and is equipped with a water jacket to allow for precise temperature control. The light emitted by the lamp passes through a lens assembly (77330, Newport) focusing the beam on the reactor window, an H_2O filter (61945, Newport) and a 385 nm cut-off optical filter. A KSLA gas pump is applied to ensure a sufficient mixing of gases in the headspace of the reactor and the stainless-steel tubes (2.5 mL·min^{-1} continuous operation). Every 60 min a probe of the headspace is analysed by the GC. In a typical experiment 30.0 mg MOF were suspended in 23.5 mL CH_3CN, 4.7 mL TEA and 0.5 mL H_2O. The suspension was then placed in the reactor and deoxygenated by an argon flow of 30 mL·mi n^{-1} applied for 30 min at 25 ^{o}C. The oxygen concentration was monitored by the GC analysis. Once the system is free of oxygen, the illumination is turned on with concomitant GC analysis (CP 9001 gas chromatograph, Chrompack)

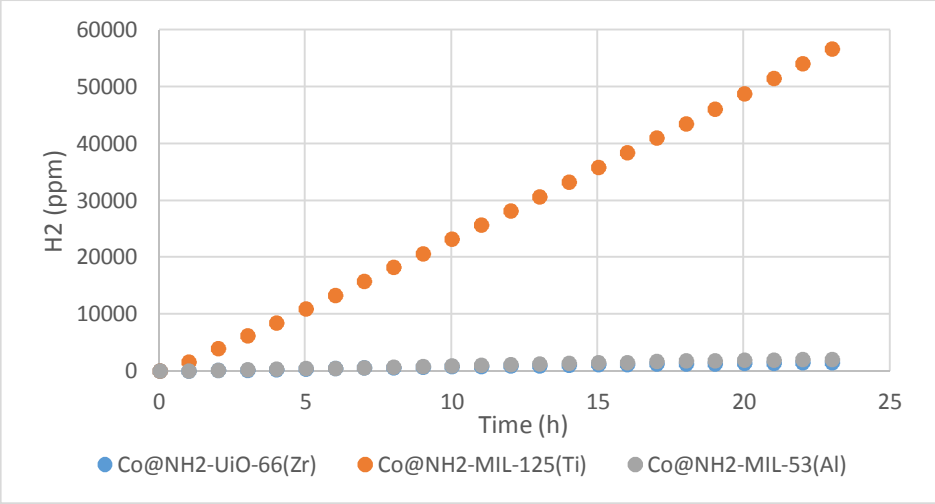

Fig. S10. H_2 generation evolution upon illumination with ligh > 385 nm of different MOFs featuring different metallic nodes (specified in brackets) loaded with Co^{2+} species and the oxime ligand.

1. A. Caballero, A. O. González-Elipe, A. Fernandez, J.-M. Herrmann, H. Dexpert, F. J. Villain, *Photochem. Photobiol. A Chem.* 1994, **78** (2), 169-172.
2. A. Fernhndez, H. Dexpert, F. Villain, *J. Phys.Chem*. 1995, **99**, 3303-3309.
3. G. Smolentsev, A. A. Guda, M. Janousch, C. Frieh, G. Jud, F. Zamponi, M. Chavarot-Kerlidou, V. Artero, J. A. van Bokhoven, M. Nachtegaal, *Faraday Discuss.* 2014, **171** (Scheme 1), 259-273.
4. T. Li Hsiung, H. P. Wang, Y. M. Lu, M. C. Hsiao, *Radiat. Phys. Chem.* 2006, **75** (11), 2054- 2057.
5. O. Mathon, A. Beteva, J. Borrel, D. Bugnazet, S. Gatla, R. Hino, I. Kantor, T. Mairs, M. Munoz, S. Pasternak, F. Perrin, S. Pascarelli, *J. Synchrotron Rad.* 2015, **22**, 1548–1554.
6. B. Ravel, M. Newville, *J. Synchrotron Rad*. 2005, **12**, 537–541.
7. M. A. Nasalevich, R. Becker, E. V. Ramos-Fernandez, S. Castellanos, S. L. Veber, M. V. Fedin, F. Kapteijn, J. N. H. Reek, J. I. van der Vlugt and J. Gascon, *Energy Environ. Sci*., 2015, **8**, 364-375.